PCP
PLANT & CELL PHYSIOLOGY

A Sodium Transporter HvHKT1;1 Confers Salt Tolerance in Barley via Regulating Tissue and Cell Ion Homeostasis

Yong Han[1], Shuya Yin[1], Lu Huang[1], Xuelong Wu[1], Jianbin Zeng[1], Xiaohui Liu[2], Long Qiu[1], Rana Munns[3], Zhong-Hua Chen[1,2] and Guoping Zhang[1,*]

[1]Agronomy Department, Key Laboratory of Crop Germplasm Resource of Zhejiang Province, Zhejiang University, Hangzhou 310058, China
[2]School of Science and Health, Hawkesbury Institute for the Environment, Western Sydney University, Penrith, NSW 2751, Australia
[3]Australian Research Council Centre of Excellence in Plant Energy Biology and School of Agriculture and Environment, University of Western Australia, Crawley, WA 6009, Australia
*Corresponding author: E-mail, zhanggp@zju.edu.cn; Fax, +86-571-88982115.
(Received January 15, 2018; Accepted June 10, 2018)

Regular Paper

Our previous studies showed that high salt tolerance in Tibetan wild barley accessions was associated with HvHKT1;1, a member of the high-affinity potassium transporter family. However, molecular mechanisms of HvHKT1;1 for salt tolerance and its roles in K^+/Na^+ homeostasis remain to be elucidated. Functional characterization of HvHKT1;1 was conducted in the present study. NaCl-induced transcripts of *HvHKT1;1* were significantly higher in the roots of Tibetan wild barley XZ16 relative to other genotypes, being closely associated with its higher biomass and lower tissue Na^+ content under salt stress. Heterologous expression of *HvHKT1;1* in *Saccharomyces cerevisiae* (yeast) and *Xenopus laevis* oocytes showed that HvHKT1;1 had higher selectivity for Na^+ over K^+ and other monovalent cations. HvHKT1;1 was found to be localized at the cell plasma membrane of root stele and epidermis. Knock-down of *HvHKT1;1* in barley led to higher Na^+ accumulation in both roots and leaves, while overexpression of *HvHKT1;1* in salt-sensitive Arabidopsis *hkt1-4* and *sos1-12* loss-of-function lines resulted in significantly less shoot and root Na^+ accumulation. Additionally, microelectrode ion flux measurements and root elongation assay revealed that the transgenic Arabidopsis plants exhibited a remarkable capacity for regulation of Na^+, K^+, Ca^{2+} and H^+ homeostasis under salt stress. These results indicate that HvHKT1;1 is critical in radial root Na^+ transport, which eventually reduces shoot Na^+ accumulation. Additionally, HvHKT1;1 may be indirectly involved in retention of K^+ and Ca^{2+} in root cells, which also improves plant salt tolerance.

Keywords: Heterologous expression • HKT transporter • *Hordeum vulgare* • Ion homeostasis • Salt stress • Sodium detoxification.

Abbreviations: AP, arginine phosphate; BSMV, *Barley stripe mosaic virus*; HKT, high-affinity potassium transporter; ICP-OES, inductively coupled plasma-optical emission spectrometry; MIFE, microelectrode ion flux estimation; NSCC, non-selective cation channel; PBS, phosphate-buffered saline; qRT-PCR, quantitative real-time PCR; RT–PCR, reverse transcription PCR; sGFP, superfolder green fluorescent protein; SOS, salt overly sensitive; VIGS, virus-induced gene silencing.

Introduction

Soil salinity is a major abiotic stress limiting crop production worldwide (FAO, http://www.fao.org/tc/exact/sustainable-agriculture-platform-pilot-website/soil-salinity-management/en (June 29, 2018, date last accessed), Rengasamy 2010). Development of salt-tolerant crops is an effective approach for better utilization of saline soil. Salinity tolerance in plants is a polygenic trait with contributions from developmental, physiological and environmental interactions. The molecular and physiological mechanisms of plant salt tolerance have been intensively investigated, with most of the studies being focused on avoiding Na^+ toxicity while maintaining sufficient ion concentrations for osmotic adjustment to the soil salinity (Munns and Tester 2008). Barley (*Hordeum vulgare* L.) is one of the most salt-tolerant cereal crops, but genotypes differ in tolerance level. For example, seedlings of a barley cultivar California Mariout (CM) showed no growth retardation under salt stress, while other genotypes were seriously inhibited (Epstein et al. 1980). Meanwhile, some Tibetan wild barley (*Hordeum vulgare* spp. *spontaneum*) accessions (e.g. XZ16 and XZ26) have been found to be even more tolerant to salinity than cultivated barley (Qiu et al. 2011, Wu et al. 2011).

The two high-affinity potassium transporter (HKT) subfamilies HKT1 and HKT2 are involved in ion homeostasis and adaptation to salt stress (Corratgé-Faillie et al. 2010, Sassi et al. 2012), so understanding the salinity-tolerant mechanisms of these plasma membrane transporters is crucial for breeding approaches to enhance the salt tolerance of crops (Hauser and Horie 2010). The serine residue (SGGG-type) in the first p-loop region primarily determines the Na^+ permeability of subfamily I HKT transporters (Mäser et al. 2002a, Mäser et al. 2002b, Horie et al. 2009). Nonetheless, in-depth functional predictions of HKT genes need to be supported by their expression patterns and ion specificities, in addition to sequence comparisons (Mäser et al. 2002b). This is particularly important in the major cereal crops such as wheat, rice and barley, which have multiple HKT-encoding genes (Huang et al. 2008, Horie et al. 2009, Waters et al. 2013).

The Arabidopsis genome possesses only one HKT belonging to subfamily I (Mäser et al. 2001), which is Na^+ selective and expressed in the xylem parenchyma, and retrieves Na^+ as it

Plant Cell Physiol. 59(10): 1976–1989 (2018) doi:10.1093/pcp/pcy116, Advance Access publication on 15 June 2018, available online at www.pcp.oxfordjournals.org

flows towards the leaves (Uozumi et al. 2000, Kato et al. 2001, Mäser et al. 2002a, Mäser et al. 2002c). Analogous mechanisms have been demonstrated for HKT1;4 and HKT1;5 in wheat and rice (Huang et al. 2006, Byrt et al. 2007, Byrt et al. 2014, Suzuki et al. 2016, Kobayashi et al. 2017). In contrast, specific subfamily II HKT transporters mediate cation influx into roots, particularly K^+ (Horie et al. 2007). In barley, previous studies on the Tibetan wild barley accessions showed that salt tolerance was associated with allelic variation in two genes: *HvHKT1* and *HvHKT2* (Qiu et al. 2011). Many SNPs were detected in the genomic sequence of *HvHKT1* from 40 barley representatives differing in salt tolerance, which were statistically associated with barley root Na^+ and shoot K^+ content under salinity (Qiu et al. 2011). However, this observation did not provide any direct evidence of its role in salt tolerance, or a detailed functional comparison with other plant HKTs. Comparatively, HvHKT2; 1 has been functionally characterized by Mian et al. (2011), and found to be a Na^+/K^+ co-transporter that increases salt tolerance by reinforcing the salt-including behavior in barley.

HvHKT1 is renamed HvHKT1;1 here, because it was annotated first (GenBank: JF496205.1, Qiu et al. 2011) and belongs to the same cluster as AtHKT1;1 and OsHKT1;1 based on their phylogeny. We hypothesize that HvHKT1;1 confers salt tolerance via direct regulation of Na^+ and indirect regulation of K^+, Ca^{2+} and H^+ homeostasis in plant cells. In the present study, the gene encoding HvHKT1;1 was expressed in *Saccharomyces cerevisiae* and *Xenopus laevis* oocytes to investigate its ion transport properties. Immunofluorescence assays and confocal microscopy were performed to identify its cell type localization. Transgenic approaches including transient virus-induced gene silencing (VIGS) and constitutive expression were also employed to dissect the function of HvHKT1;1 in plants.

Results

NaCl induces high expression of *HvHKT1;1* in salt-tolerant Tibetan wild barley

Two cultivated barley genotypes CM72 and Gairdner (salt tolerant and sensitive, respectively), and two Tibetan wild barley accessions XZ16 and XZ169 (salt tolerant and sensitive, respectively) differing in salt tolerance (Chen et al. 2005, Wu et al. 2011) were used. Under 300 mM NaCl, salt-tolerant Tibetan wild barley XZ16 showed only a 14% reduction in dry biomass compared with the control (**Fig. 1a**), whilst a reduction of 51% was found in the salt-tolerant cultivar CM72. In addition, XZ16 accumulated less Na^+ in the roots and shoots than the other wild or cultivated genotypes (**Fig. 1b, c**). Generally, expression of *HvHKT1;1* was up-regulated in response to the salinity shock in all plant tissues of four barley genotypes, and it was preferentially expressed in roots (**Fig. 1d**), with lower expression levels in leaves and sheaths (**Fig. 1e, f**). The *HvHKT1;1* expression increased in roots of all genotypes exposed to 150 mM NaCl for 2 h, with XZ16 having a >19-fold increase (**Fig. 1d**). The rapid up-regulation of root *HvHKT1;1* expression was closely associated with higher relative plant dry biomass, lower tissue Na^+ content and a lower root Na^+/K^+ ratio in all four barley genotypes under salinity stress (Supplementary Table S1).

HvHKT1;1 is a Na^+ transporter

Phylogenetic analysis, yeast heterologous expression and two-electrode voltage clamp in oocytes all validated that HvHKT1;1 is a Na^+ transporter (**Figs. 2 and 3**). HvHKT1;1 cloned from XZ16 exhibited 41% sequence identity to AtHKT1;1, and was highly homologous (60% sequence identity) to rice OsHKT1;1 and OsHKT1;2 (**Fig. 2a;** Supplementary Table S2). Furthermore, there are five conserved amino acid polymorphisms at the 55th S/C, 198th Q/H, 204th A/T, 254th I/V and 522th V/L positions (Supplementary Fig. S1) between salt-tolerant (XZ16 and CM72) and -sensitive (XZ169, Gairdner and Bowman) barley genotypes, respectively. Comparative analysis of the amino acid sequence and prediction of the transmembrane structure revealed a conserved Ser128 at the first p-loop amongst HvHKT1;1 variants (Supplementary Fig. S1), suggesting that HvHKT1;1 is likely to be Na^+ permeable.

A yeast complementation experiment was conducted to reveal the ion specificity of HvHKT1;1 (**Fig. 2b**). The yeast mutant R5421 (Δ*trk1* Δ*trk2*) lacking endogenous K^+ uptake systems was transformed with *HvHKT1;1* or an empty vector control, and then grown on arginine phosphate (AP) agar plates with additional K^+/Na^+ supplementation. Under low external K^+ ($[K^+]_{ext} < 1$ mM), the growth of *HvHKT1;1*-expressing yeast was similar to that of the empty vector control, but was unable to recover the growth of R5421 compared with the wild-type strain R757 having functional TRK transporters, indicating its low affinity for K^+ (**Fig. 2b**). Elevating $[K^+]_{ext}$ to 10 mM rescued the normal growth of R5421 as well as the yeast transformed with *HvHKT1;1* or vector control (**Fig. 2b**). To determine further whether HvHKT1;1 is Na^+ permeable, an additional 100 mM NaCl was added to the plates and only the growth of *HvHKT1;1*-expressing yeast was significantly inhibited (**Fig. 2b**). From these results, it is apparent that HvHKT1;1 is most likely to form a Na^+- but not K^+-permeable transporter.

To investigate further the transport properties, two-electrode voltage-clamp assays were performed on *HvHKT1;1*-cRNA-injected *X. laevis* oocytes (**Fig. 3**). Significant inward currents were only observed for *HvHKT1;1*-expressing oocytes in the presence of 100 mM Na^+, with a reversal potential (E_{rev}) of around −20 mV (**Fig. 3a**). Replacing external Na^+ with 100 mM of other monovalent cations including K^+, Li^+, Rb^+, Cs^+ and $Tris^+$ resulted in a more negative E_{rev} of around −80 mV, and no significant inward current was detected at a physiological range of membrane voltages (**Fig. 3a**). A 10-fold increase in external Na^+ concentration ($[Na^+]_{ext}$), from 1 to 10 mM, gave rise to a 47.9 mV increase on average in the E_{rev} and a further 28.8 mV increase on average in response to an increase in $[Na^+]_{ext}$ from 10 to 30 mM (**Fig. 3b**). These are close to the predicted shifts in membrane potential based on Nernst potential calculations for Na^+ (E_{Na}; 59 and 26 mV, respectively). In contrast, there were no significant inward currents detected in various concentrations of $[K^+]_{ext}$ (**Fig. 3b**). This evidence suggests that HvHKT1;1 forms a Na^+- but not a K^+-permeable

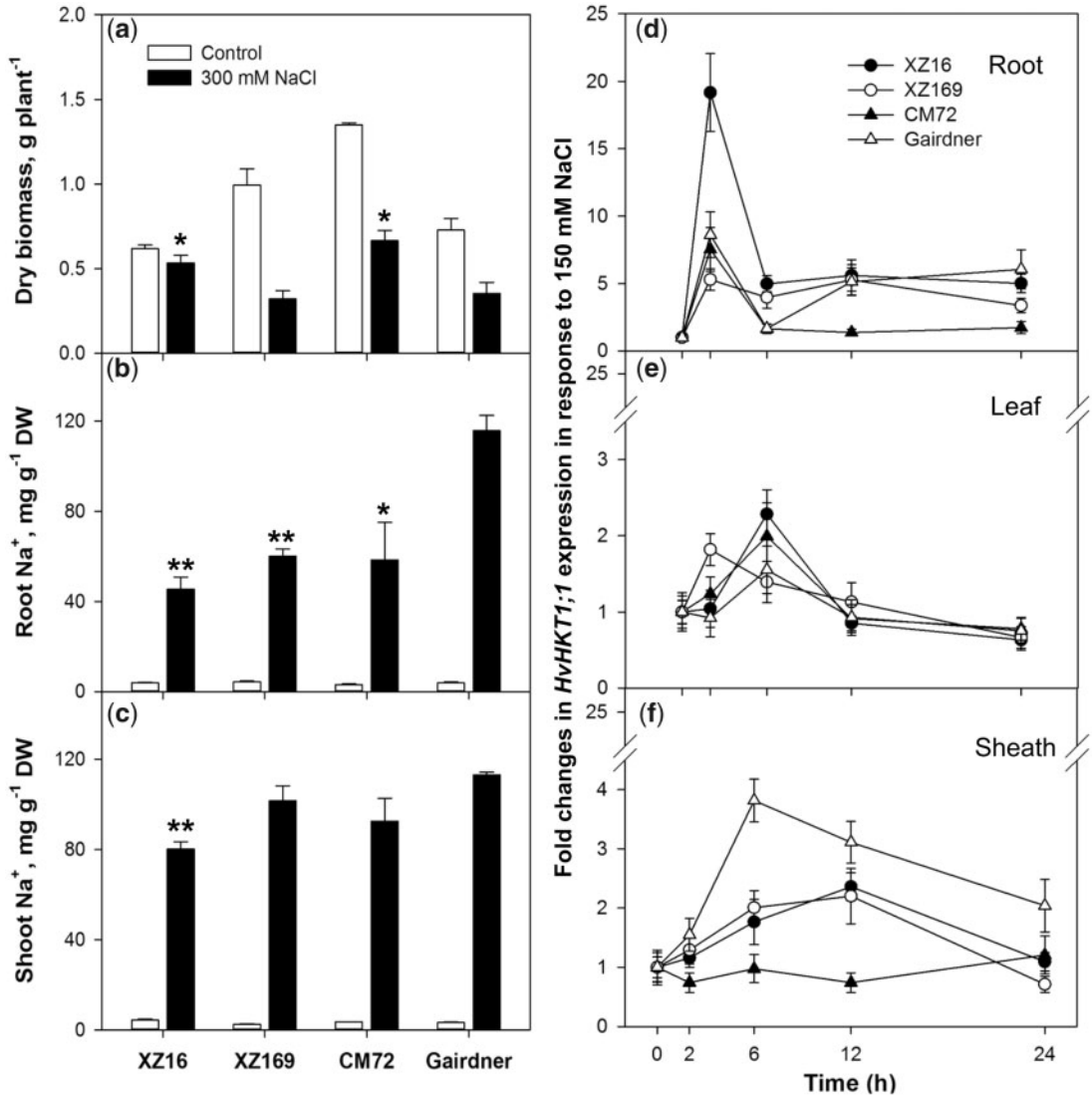

Fig. 1 Physiological responses and time-course *HvHKT1;1* transcript levels in representative barley genotypes under salt treatment. (a–c) Dry biomass, root Na^+ and shoot Na^+ concentrations in the control and salt treatment with 300 mM NaCl for 17 d. Asterisks denote values that were significantly different from those of Gairdner by one-way ANOVA (*$P < 0.05$; **$P < 0.01$). Data are means ± SE ($n = 3$). (d–f) Dynamic expression of *HvHKT1;1* in barley root, leaf and sheath in response to salt treatment. Plants were grown hydroponically and samples were collected at 0, 2, 6, 12 and 24 h after 150 mM NaCl stress for qRT-PCR. *Gapdh* was used as a reference gene. Fold changes in *HvHKT1;1* expression are all normalized to the time point 0 h (control) for each genotype using the $2^{-\Delta\Delta Ct}$ method. Values are means ± SD ($n = 6$).

transporter. However, Na^+ transport through HvHKT1;1 was inhibited by the presence of K^+ (**Fig. 3c**). Significant reductions in the magnitude of the inward currents, but not outward currents, were observed in both low and high $[Na^+]_{ext}$, when $[K^+]_{ext}$ was elevated from 0 to 10 mM (**Fig. 3c, d**).

HvHKT1;1 is localized on the plasma membrane and is specifically expressed in root stele and epidermis

To confirm whether HvHKT1;1 is a plasma membrane transporter, its subcellular localization was investigated by expressing *HvHKT1;1::sGFP* in onion epidermal cells. Green fluorescence was only detected on the plasma membrane, as indicated by its co-localization with a plasma membrane marker emitting red fluorescence (**Fig. 4a**). As *HvHKT1;1* mRNA expression was mainly induced in the roots under salt treatment, but not the leaves and sheaths of barley (**Fig. 1d–f**), the tissue-specific expression of *HvHKT1;1* was investigated only in roots from two barley genotypes by immunofluorescence. After pre-treatment of barley roots in 150 mM NaCl for 16 h, the expression of *HvHKT1;1* was predominantly observed in the stele and epidermis for the salt-tolerant genotype XZ16, particularly on the xylem walls and parenchyma cells adjacent to the xylem vessels (**Fig. 4b**). Similar results were found in the other wild barley accession (XZ169) which is salt susceptible (Supplementary Fig. S2).

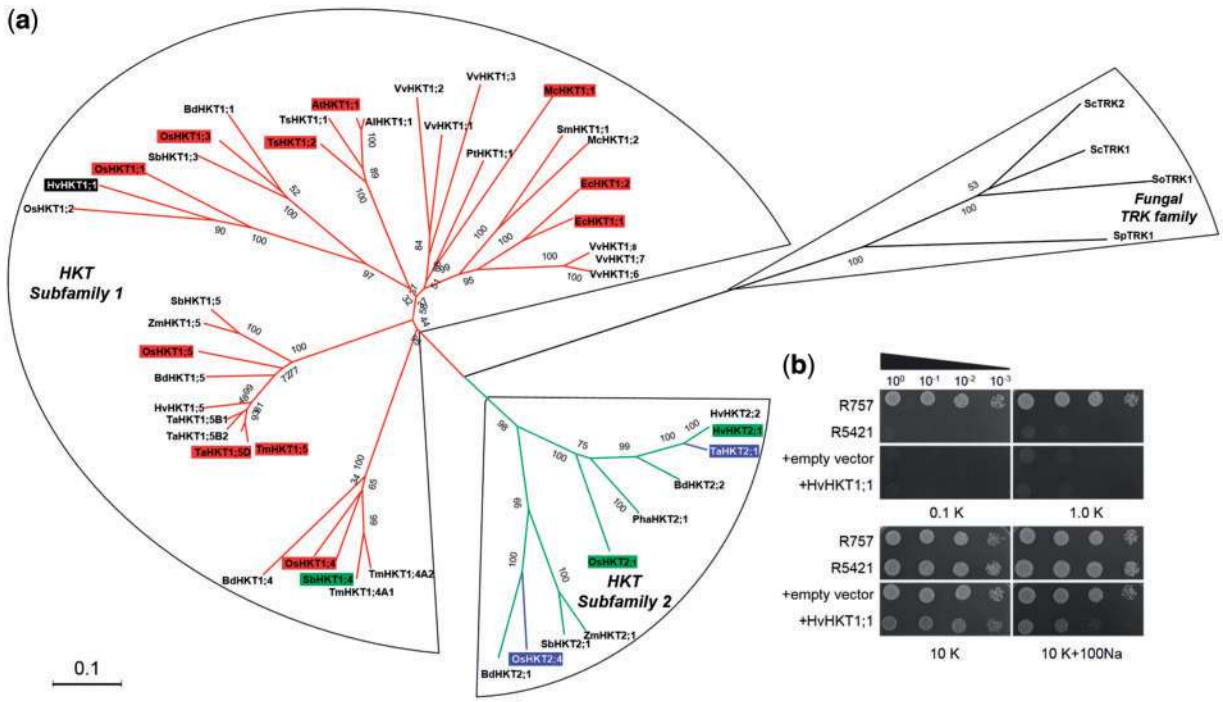

Fig. 2 Phylogenetic analysis and functional characterization of HvHKT1;1 in *S. cerevisiae*. (a) Unrooted minimum-evolution phylogenetic tree of plant HKT transporters. The diagram illustrates two major HKT subfamilies, and TRKs represent the outgroup. The subfamily I HKT transporters facilitating Na^+ removal from xylem vessels are shaded in red. The proteins shaded in green are proven to be Na^+/K^+ co-transporters, which mainly belong to subfamily II. The proteins shaded in blue indicate a role in Ca^{2+} transport. The transport functions of the remaining HKT proteins are not identified at yet, including HvHKT1;1 that is shaded in black. Accession numbers for gene names can be found in Supplementary Table S2. The scale bar indicates 0.1 substitutions per site. Abbreviations: *At*, *Arabidopsis thaliana*; *Al*, *Arabidopsis lyrata*; *Bd*, *Brachypodium distachyon*; *Ec*, *Eucalyptus camaldulensis*; *Hv*, *Hordeum vulgare*; *Mc*, *Mesembryanthemum crystallinum*; *Os*, *Oryza sativa*; *Pha*, *Phragmites australis*; *Pt*, *Populus trichocarpa*; *Sm*, *Selaginella moellendorffii*; *Ta*, *Triticum aestivum*; *Tm*, *Triticum monoccocum*; *Ts*, *Thellungiella salsugenia*; *Vv*, *Vitis vinifera*; *Zm*, *Zea mays*. (b) Ectopic expression of *HvHKT1;1* in the *S. cerevisiae* strain R5421 (*Δtrk1 Δtrk2*) lacking an endogenous K^+ uptake system. Yeast R5421 and that harboring the vector control *pYES2.0* or *pYES2::HvHKT1;1* were spotted in decimal dilutions on AP medium (Rodríguez-Navarro and Ramos 1984) containing additional K^+ and Na^+ with the indicated concentrations (mM). The wild-type yeast strain R757 was used as a positive control. Plates were incubated at 30°C for 5 d and then photographed.

Silencing of *HvHKT1;1* leads to higher Na^+ accumulation in barley leaf and root

First, the barley *phytoene desaturase* (*PDS*) gene was used as a marker to verify the VIGS effect in wild barley XZ16. BSMV:*HvPDS* plants showed photobleaching symptoms after infection, indicating that *Barley stripe mosaic virus* (BSMV)-induced silencing of *HvPDS* had been successfully achieved in the genotype XZ16 (Supplementary Fig. S3). Thereafter, the VIGS system was used for knock-down of *HvHKT1;1* in the salt-tolerant XZ16. Compared with BSMV:γ plants, the emergence of young leaves was inhibited in the BSMV:*HvHKT1;1* plants, resulting in a significant reduction in dry biomass when grown in hydroponic solution with an additional 200 mM NaCl (**Fig. 5a**). Moreover, BSMV:*HvHKT1;1* plants accumulated more Na^+ but less K^+ in shoots than BSMV:γ plants under both control and saline conditions (**Fig. 5b**). Most importantly, BSMV:*HvHKT1;1* plants had significantly higher Na^+ content and significantly lower K^+ content in roots than BSMV:γ plants with no additional NaCl, but this difference was diminished after 200 mM NaCl treatment for 5 d (**Fig. 5b**). Transcription of *HvHKT1;1* was enhanced in roots of BSMV:γ plants in response to salt shock, in line with previous results (**Fig. 1d**). However, the transcripts were significantly reduced in roots of BSMV:*HvHKT1;1* plants, by an average of 88% at 1.5, 6 and 24 h of salt treatment relative to the BSMV:γ plants (**Fig. 5c**). Although *HvHKT1;1* expression was not highly induced in shoots of BSMV:γ plants under salt treatment, it was almost completely knocked-down in BSMV:*HvHKT1;1* plants (**Fig. 5c**). BSMV-mediated knock-down of *HvHKT1;1* transcription was further proved by Western blot, as the HvHKT1;1 protein content in roots was much lower in BSMV:*HvHKT1;1* plants than in BSMV:γ plants after 5 d salt treatment (**Fig. 5d**).

HvHKT1;1 alleviates growth inhibition of salt-sensitive Arabidopsis mutants by regulating K^+, Na^+ and Ca^{2+} homeostasis

Based on the phylogenetic analysis and *HvHKT1;1* heterologous expression, it appeared that constitutive expression of *HvHKT1;1* is unlikely to improve plant salt tolerance because

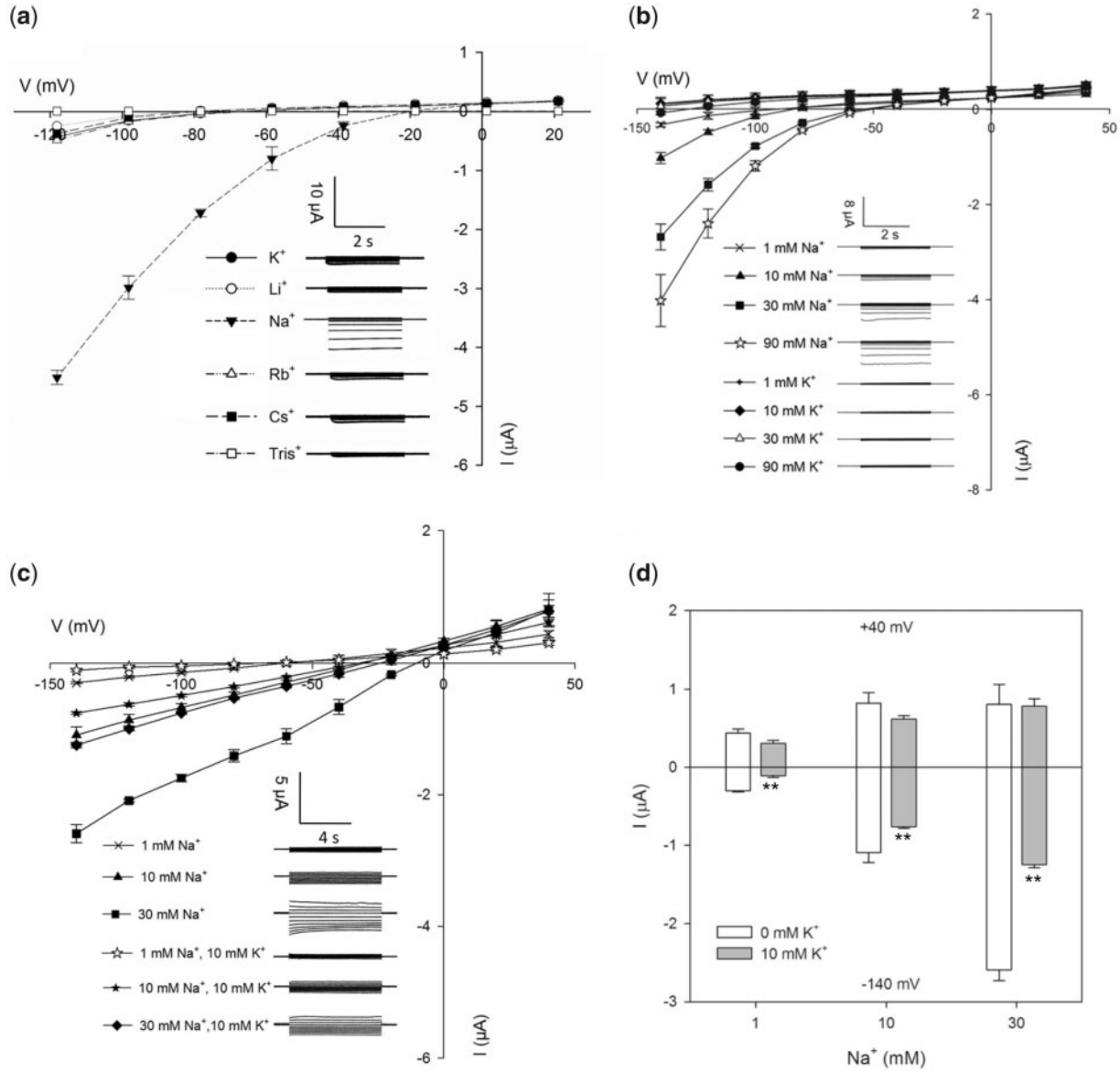

Fig. 3 Characterization of HvHKT1;1 in *Xenopus laevis* oocytes. (a) Current–voltage (I–V) curves for HvHKT1;1-expressing oocytes clamped in a series of 100 mM monovalent cations. (b) HvHKT1;1 conductance in varying external concentrations of Na^+ and K^+. (c) I–V curves for *HvHKT1;1*-cRNA-injected oocytes bathed in solutions containing 1, 10 or 30 mM Na^+ with or without additional 10 mM K^+. (d) Currents of *HvHKT1;1*-expressing oocytes clamped at 40 mV or −140 mV in serial Na^+ or Na^+ and K^+ solutions (**$P < 0.01$). Average current profiles were obtained from *HvHKT1;1*-cRNA-injected oocytes, 3 d after injection, with voltage steps applied from +40 to −140 in 20 mV steps and a holding potential of −20 mV. Values are means ± SE ($n = 4$).

it causes overaccumulation of Na^+ in shoots of wild-type Arabidopsis (Møller et al. 2009, Wang et al. 2014). Therefore, we investigated the roles of HvHKT1;1 in Arabidopsis *hkt1* and *sos1* mutants (Supplementary Fig. S4).

The *HvHKT1;1*-overexpressing lines 12-5 (from mutant *hkt1-4*), 29-1/37-3 (from mutant *sos1-6*) and 59-6/77-6 (from mutant *sos1-12*) all displayed significantly ($P < 0.05$) lower growth reductions compared with their corresponding mutants under salt stress (**Fig. 6a–f**). Hence, we selected these three representative lines (12-5, 29-1 and 77-6) for further functional analysis of HvHKT1;1. Na^+, K^+ and Ca^{2+} contents were measured in wild-type, loss-of-function and transgenic lines in response to NaCl treatment (**Fig. 6g–i**). Na^+ concentration differed significantly between the loss-of-function and overexpression lines. For instance, *hkt1-4* and *sos1-12* had 65% and 95% higher shoot Na^+ concentrations than the wild-type (Col-0), respectively. However, overexpression of *HvHKT1;1* in the mutants significantly ($P < 0.01$) reduced shoot Na^+ in 12-5 and 77-6 to levels close to that of Col-0 (**Fig. 6g**). Notably, Na^+ concentrations in the roots of *hkt1-4* and 12-5 were quite low, being 12.4 and 9.6 mg g^{-1} DW, respectively (**Fig. 6h**). Surprisingly, *HvHKT1;1*-overexpressing lines exhibited significantly higher relative K^+ and Ca^{2+} concentrations under salinity stress (**Fig. 6i**).

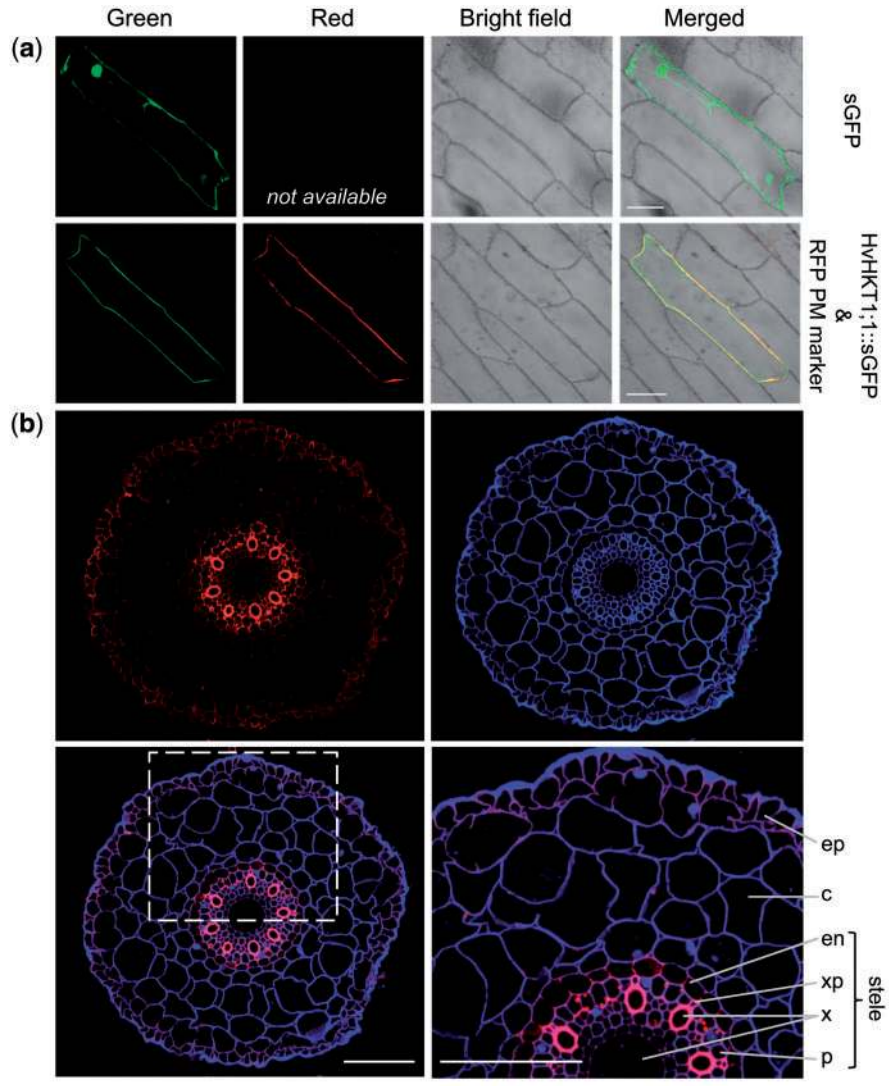

Fig. 4 Localization of HvHKT1;1 *in planta*. (a) Subcellular localization of HvHKT1;1 in onion epidermis cells. The upper layer shows representative images of particle-mediated transient expression of sGFP alone (as control), and the lower layer shows co-expression of HvHKT1;1::sGFP and a red fluorescent protein (RFP) plasma membrane marker. Panels in each column show the captured signal of green (GFP), red (RFP), bright field and merged channels. (b) Cell type localization of HvHKT1;1 in barley roots. Immunostaining with an anti-HvHKT1;1 antibody was performed 5 mm from the root apex of XZ16 after 7 d germination. Roots were exposed for 16 h to 2.0 mM K^+, 0.5 mM Ca^{2+} and 150 mM Na^+ before sampling. Red fluorescence shows the presence of HvHKT1;1 and blue fluorescence is emitted by the counterstain DAPI. Cell types are indicated in the enlarged panel with merged signals. c, cortex; en, endodermis; ep, epidermis; p, pericycle; x, xylem; xp, xylem parenchyma. Scale bars = 100 μm.

HvHKT1;1 regulates K^+, H^+ and Ca^{2+} fluxes and root growth under salt stress

Microelectrode ion flux estimation (MIFE) provided further evidence that HvHKT1;1 could take part in the regulation of Na^+, K^+ and Ca^{2+} homeostasis in Arabidopsis in response to salt stress (**Fig. 7**). Imposition of NaCl stress resulted in a significant transient K^+, H^+ and Ca^{2+} efflux from all seven lines over the duration of 40 min flux measurements (**Fig. 7**). Importantly, the NaCl-induced transient and steady-state K^+ and Ca^{2+} effluxes were significantly lower in the three transgenic lines than in their corresponding loss-of-function mutants and Col-0 (**Fig. 7a, c**). Only the transient and steady-state net H^+ effluxes of *sos1-12* were significantly ($P < 0.01$) larger than that of the other lines (**Fig. 7b**). In addition, K^+ and H^+ fluxes of the seven lines were significantly correlated to the measured Na^+ accumulation and plant biomass after salt treatment (**Table 1**).

We also conducted a comprehensive set of root growth experiments using different external Na^+, K^+ and Ca^{2+} concentrations (Supplementary Fig. S5; Table S3). There was no significant difference in root length between *HvHKT1;1* overexpression lines and their corresponding mutants under control conditions. However, increasing Na^+ to a moderate

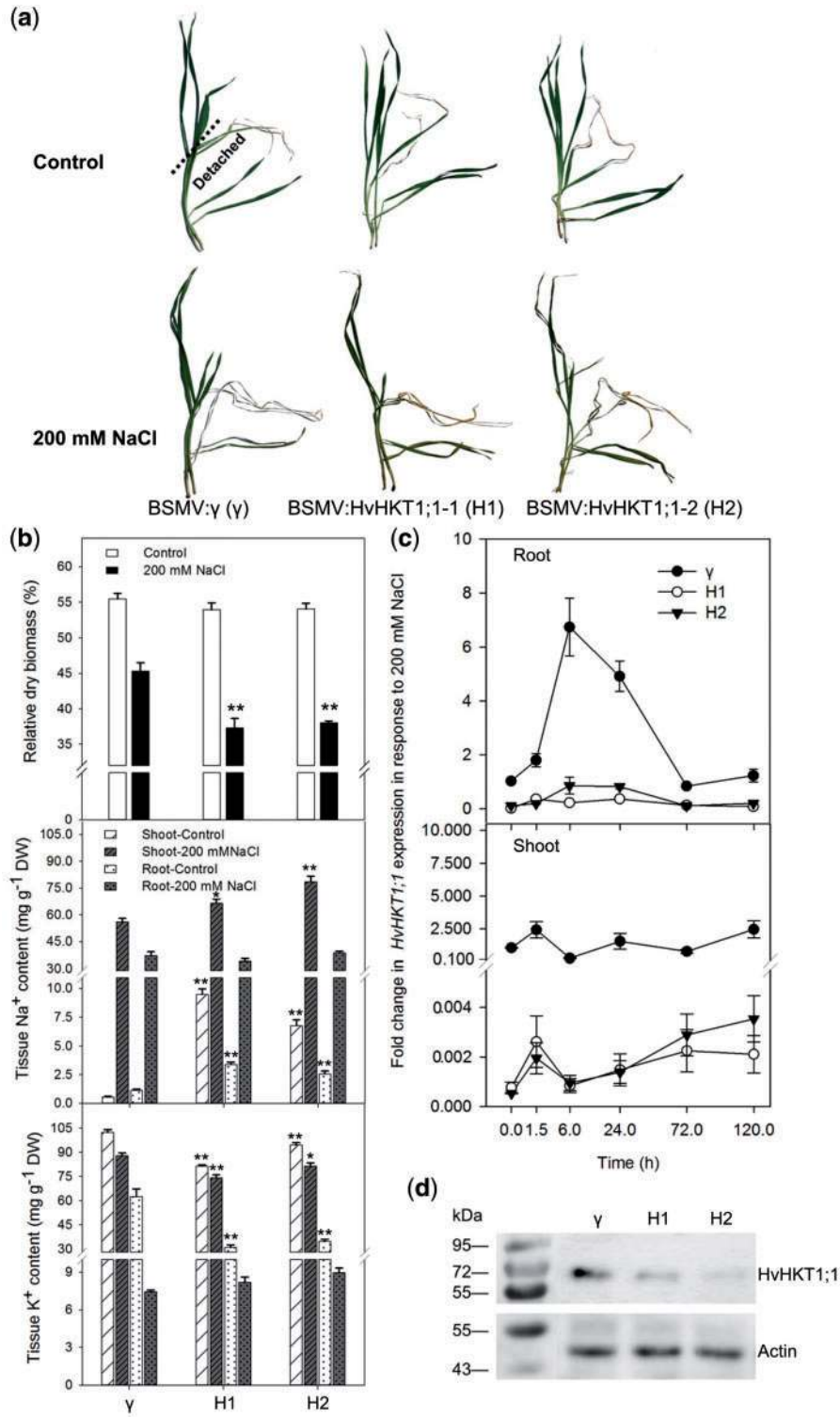

Fig. 5 Functional characterization of HvHKT1;1 in wild barley XZ16 via BSMV-VIGS. (a) Representative BSMV:γ (γ, vector control) and BSMV:*HvHKT1;1* (H1 and H2 for two interfering fragments) plants after salt treatment. Barley plants were grown in aerated hydroponics and inoculated with *in vitro* transcribed RNA at the two-leaf stage, and then treated with (treatment) or without (control) an additional 200 mM NaCl 14 d after inoculation. Plant tissues above the inoculated leaf were detached from the main shoot for dry biomass quantification. (b) Relative dry biomass (the biomass of detached leaves divided by the value of whole plant shoots), tissue Na^+ and K^+ contents. Data are means ± SE ($n = 8$). * and ** indicate significant differences between BSMV:γ and BSMV:*HvHKT1;1* at $P < 0.05$ and $P < 0.01$, respectively. (c) Dynamic expression of *HvHKT1;1* in barley BSMV plants under salt treatment. *18S rRNA* and *β-tubulin* were used as internal controls. Fold changes in tissue *HvHKT1;1* expression are all normalized to the BSMV:γ plants at the time point of 0 h using the $2^{-\Delta\Delta Ct}$ method. Values are means ± SD ($n = 6$). (d) HvHKT1;1 immunoblotting from the root of BSMV:γ and BSMV:*HvHKT1;1* plants after 5 d salt treatment. Actin was used as loading control.

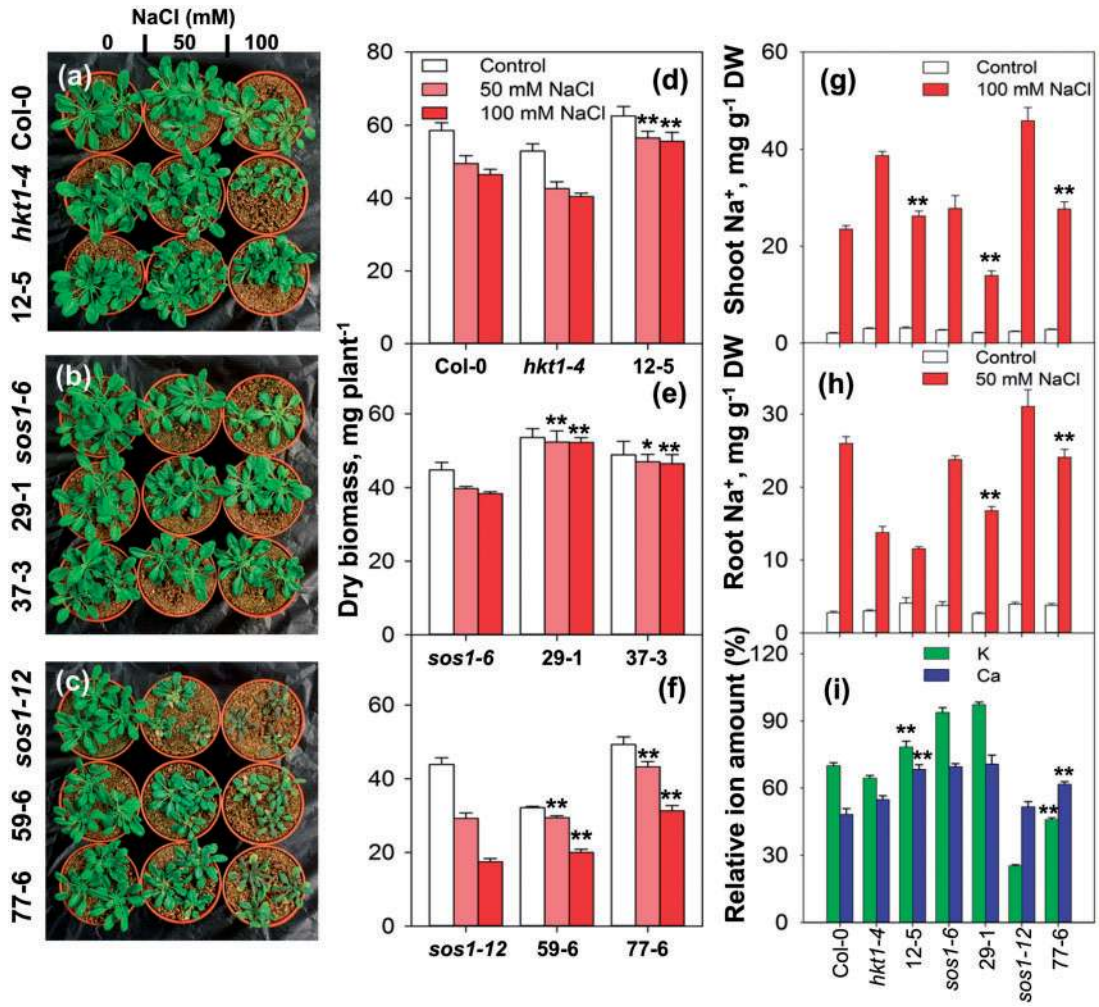

Fig. 6 HvHKT1;1 regulates plant growth and ionic response of Arabidopsis *hkt1* and *sos1* mutants to salt stress. Four-week-old vermiculite-grown Arabidopsis wild-type, *hkt1* and *sos1* mutants and *HvHKT1;1* overexpression lines were treated with 0, 50, and 100 mM NaCl for 14 d. (a–c) Plant growth; (d–f) dry weight; (g) and (h) Na^+ concentrations in shoot and root of representative lines; (i) relative amount of total K^+ and Ca^{2+} in shoots after treatment with 100 mM NaCl compared with corresponding control plants. Data are means ± SE ($n = 10$). * and ** indicate significant differences in relative biomass and ion contents under salt stress between overexpression lines and their parental mutants at $P < 0.05$ and $P < 0.01$, respectively.

level of 20 mM remarkably ($P < 0.05$) reduced root growth in *hkt1-4* and *sos1-12* by 22% and 63%, respectively, which was much lower than in 12-5 and 77-6 (Supplementary Fig. S5). Moreover, the transgenic lines showed significantly better root growth at low K^+ concentrations under salinity (Supplementary Table S4). For instance, 12-5 and 77-6 exhibited 89% and 41% more root growth than *hkt1-4* and *sos1-12* in 0.1 mM K^+, respectively (Supplementary Fig. S5). A 10-fold decrease in Ca^{2+} concentration significantly ($P < 0.01$) aggravated the inhibitory effect of an elevated external Na/K ratio on the root growth of all seven lines (Supplementary Table S3). Notably, transgenic lines showed 29% greater root length on average than the three loss-of-function mutants at 0.15 mM Ca^{2+}, 0.1 mM K^+ and 20 mM Na^+ (Supplementary Fig. S5). These results further indicated that HvHKT1;1 affected Na^+, K^+ and Ca^{2+} homeostasis and plant growth under salt stress.

Discussion

Diverse functions of HKTs contribute to the salt tolerance of cereal crops

Functional analyses have revealed a striking diversity of HKT transporters in monocots, which could be central to the regulation of K^+ and Na^+ accumulation. With the exception of TsHKT1;2, HKT transporters permeable to both Na^+ and K^+ (subfamily II) are present predominantly in monocotyledonous species (Haro et al. 2009, Horie et al. 2009, Jabnoune et al. 2009, Hauser and Horie 2010, Suzuki et al. 2016). Structurally, HvHKT1;1 belongs to subfamily I and shows close homology to OsHKT1;1 and OsHKT1;2 (**Fig. 2a**). Interestingly, OsHKT1;1 showed outstanding capacity to transport K^+ (Jabnoune et al. 2009), but was not up-regulated in rice plants exposed to NaCl (Garciadeblás et al. 2003). OsHKT1;2 was found to be

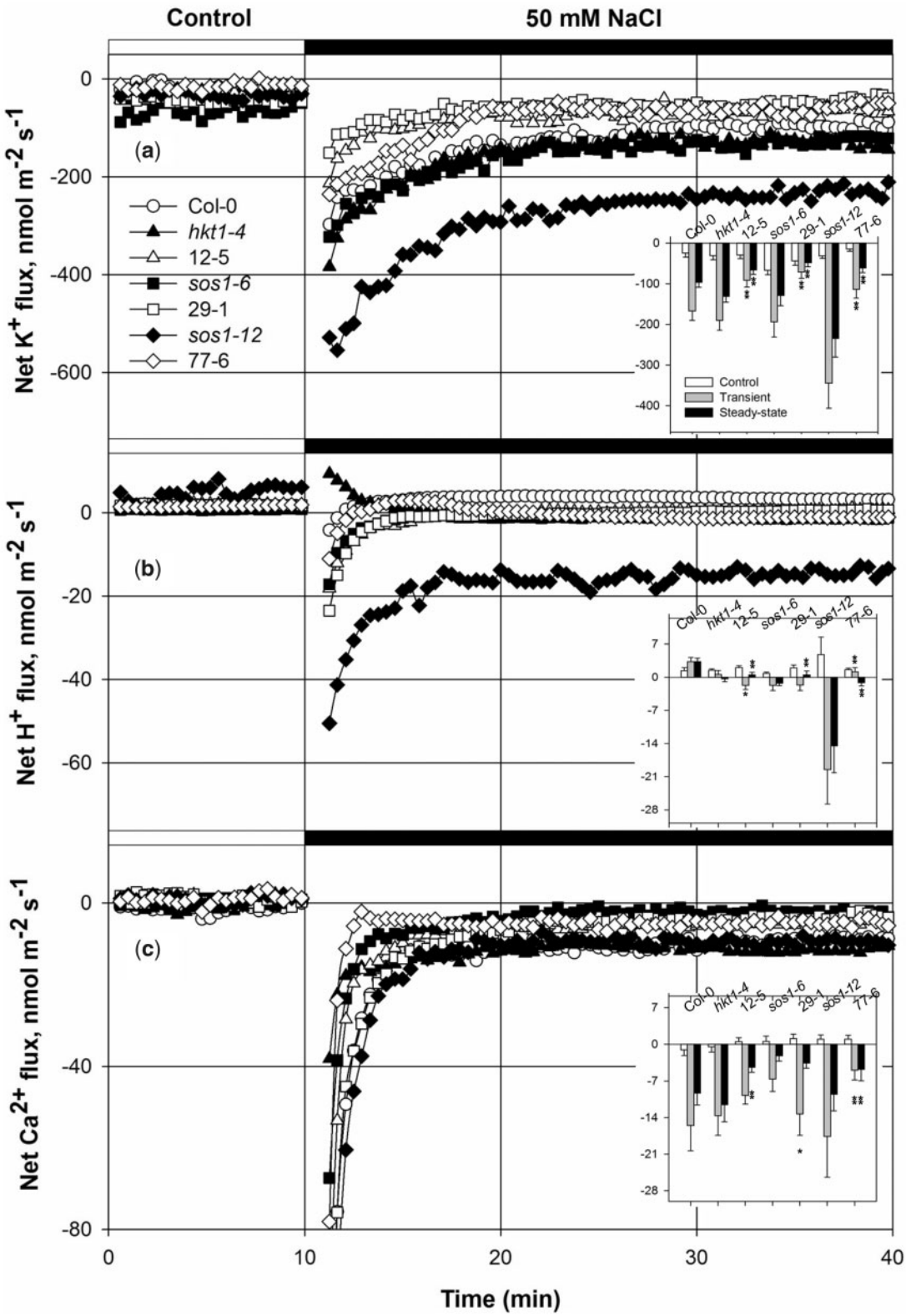

Fig. 7 NaCl-induced ion fluxes from roots of Arabidopsis wild-type, *hkt1* and *sos1* mutants and representative *HvHKT1;1* overexpression lines. Average transient K^+ (a), H^+ (b) and Ca^{2+} (c) fluxes are from the root mature zone in the control for 10 min and in 50 mM NaCl treatment for 30 min ($n = 6–10$ plants). Bar charts present the average flux data in the control (0–10 min), transient (12–22 min) and steady state (30–40 min) after salt treatment. * and ** indicate significant differences between overexpression lines and their parental mutants at $P < 0.05$ and $P < 0.01$, respectively.

Table 1 Correlation analysis between steady-state ion fluxes and tissue ion content and fresh weight of seven Arabidopsis lines under salt stress

r	Shoot Na^+	Root Na^+	Shoot K^+/Na^+ ratio	Fresh weight
K^+ flux	−0.682*	−0.885**	−0.852*	0.883**
H^+ flux	−0.778*	−0.810*	−0.728*	0.610
Ca^{2+} flux	−0.398	−0.580	−0.544	0.571

*Correlation significant at the 0.05 level.
**Correlation significant at the 0.01 level.

constitutively expressed in roots, but non-functional in the rice cultivar Nipponbare (Garciadeblás et al. 2003). However, *HvHKT1;1* expression was highly inducible under NaCl stress and showed a close correlation with salt tolerance (**Fig. 1d;** Supplementary Table S1), but it did not respond to K^+ deficiency in our transcriptome analysis in barley (Zeng et al. 2014). Our phylogenetic data even suggested that distinct clades might exist in HKT subfamily I in monocots. Further research is thus necessary to dissect the phylogenetic relationships, functional properties and regulation pathways of the HKT transporters for their roles in barley salt tolerance. In addition, certain amino acid changes may shift the transport behavior. For instance, the change of two amino acid residues in TsHKT1;2 to mimic the AtHKT1;1 sequence resulted in enhanced Na^+ uptake and loss of the TsHKT1;2 intrinsic K^+ transport activity (Ali et al. 2012). Regarding the amino acid polymorphisms in HvHKT1;1 of the salt-tolerant and -sensitive genotypes (Supplementary Fig. S1), we also postulate that some undefined functions of these amino acid residues in HKTs may be unique to halophytic plants (e.g. *Selaginella moellendorffii* and *Thellungiella salsuginea*), which differed substantially from those in glycophytic plants (e.g. rice, *Sorghum* and Arabidopsis) (Uozumi et al. 2000, Rus et al. 2004, Møller et al. 2009). Hence, it is of great importance to uncover whether these differences in amino acid residues of HKTs contribute to higher salt tolerance in both Tibetan wild barley and transgenic Arabidopsis lines.

HvHKT1;1 belongs to subfamily I of HKT transporters and shows Na^+ specificity

Subfamily I and II HKT transporters contain either a serine (SGGG-type) or a glycine (GGGG-type) at the corresponding position in the first p-loop region (Supplementary Fig. S1). The serine residue primarily determines the Na^+ permeability of subfamily I in HKT transporters (Mäser et al. 2002a, Mäser et al. 2002b, Horie et al. 2009). However, this rule is not always followed by all HKTs. A halophytic relative of Arabidopsis, *T. salsuginea*, appears to control net Na^+ and K^+ uptake tightly through TsHKT1;2, which shows K^+ specificity in the presence of NaCl (Volkov and Amtmann 2006, Ali et al. 2012). Similar to our results (**Fig. 1**; Supplementary Fig. S5), Ali et al. (2012) showed that the transcript of *TsHKT1;2* was strongly up-regulated by salt stress, and *athkt1;1* mutant lines overexpressing *TsHKT1;2* showed less sensitivity to K^+ deficiency in the presence of Na^+. In this study, HvHKT1;1 is a SGGG-type HKT and showed Na^+ specificity in two heterologous expression systems (**Figs. 2b, 3**). However, Na^+ transport through HvHKT1;1 is blocked by the presence of $[K^+]_{ext}$ in both low and high $[Na^+]_{ext}$ (**Fig. 3c**). Similarly, inhibition of Na^+ transport through TaHKT2;1 and OsHKT2;1 by $[K^+]_{ext}$ has been observed (Oomen et al. 2012), while this inhibition occurs only in relatively higher $[Na^+]_{ext}$ for TmHKT1;5-A and TaHKT1;5-D (Yao et al. 2010, Byrt et al. 2014). Neither phenomenon has been previously detected from *AtHKT1;1*- and *SbHKT1;4*-expressing oocytes (Uozumi et al. 2000, Wang et al. 2014). This divergence indicates differences in sensitivities of HKT proteins to $[K^+]_{ext}$ and is a matter for further investigation for physiological significance *in planta*. Given that HvHKT1;1 is Na^+ specific, it is noteworthy that decreases in tissue K^+ content under control conditions by knock-down of *HvHKT1;1* (**Fig. 5b**) could be attributed to the accumulation of Na^+ rather than a direct role for HvHKT1;1 for K^+ transport *in planta*.

Non-invasive ion flux measurement provides insights into transporter functions

Some plant HKT mRNAs such as *HvHKT2;1*, *OsHKT2;1* and *TaHKT2;1* have alternative initiations of translation when expressed in yeast and *Xenopus* oocytes, which may lead to transporters with different kinetic properties as compared with the proper forms when expressed in plants (Golldack et al. 2002, Haro et al. 2005, Haro et al. 2009, Rodríguez-Navarro and Rubio 2006). The expression of certain HKT transporters in yeast may even be toxic (Garciadeblás et al. 2003, Haro et al. 2005), making it difficult to investigate such transporters in yeast (Rodríguez-Navarro and Rubio 2006). Apart from heterologous expression in *Xenopus* oocytes and yeast, we also made use of *in planta* recordings of ion fluxes across the roots to decipher the transport properties of HvHKT1;1 in transformed Arabidopsis lines. Our results showed significant links between fluxes and K^+/Na^+ homeostasis in seven Arabidopsis lines (**Table 1**), providing insights into the functions of HvHKT1;1 in regulating diverse ion homeostasis for salt tolerance. In particular, the highest K^+ and H^+ effluxes were detected from the root of *sos1-12* in all NaCl-treated lines (**Fig. 7 a, b**). It is known that application of salt stress leads to the passive entry of Na^+ ions into the cytoplasm through non-selective cation channels (NSCCs), which results in depolarization of the plasma membrane, and thus K^+ loss (K^+ efflux) via depolarization-activated potassium outward rectifying (KOR) channels (Bose et al. 2013). Exclusion of Na^+ by the Na^+/H^+ exchanger salt overly sensitive 1 (SOS1) is critical for salinity tolerance in plants (reviewed by Munns and Tester 2008). Such energy-dependent Na^+ transport ultimately relies on a proton-motive force generated by H^+-ATPase activity (Bose et al. 2013), and physiologically this activity could be reflected by H^+ flux. NaCl-induced large H^+ efflux from *sos1-12* could be attributed to the loss of function of the Na^+/H^+ antiporter for Na^+ extrusion, which led to less H^+ influx into the cells but higher H^+ efflux (**Fig. 7b**). With respect to K^+ flux, we propose that it is indirectly affected by membrane potential and H^+/Na^+ homeostasis in the *sos1-12* mutant. The loss of

function of SOS1 reduced Na^+ exclusion, resulting in the larger NaCl-induced depolarization of the plasma membrane for higher K^+ efflux (Fig. 7a). In this study, there are profound effects on overexpression of *HvHKT1;1* in the *sos1-12* mutant. HvHKT1;1 rebuilt ion homeostasis and contributed to an elevated K^+/Na^+ ratio in 77-6 under salt stress (Fig. 6g–i), which may improve tissue salt tolerance and consequentially reduce the NaCl-induced K^+ and H^+ efflux. Our present findings revealed an indirect role for HvHKT1;1 in Ca^{2+} homeostasis; overexpressing *HvHKT1;1* significantly reduced NaCl-induced Ca^{2+} efflux (Fig. 7c), resulting in the line 77-6 retaining 10% more plant Ca^{2+} (Fig. 6i). Reduced Ca^{2+} efflux in NaCl treatment also provides evidence that HvHKT1;1 increases salt tolerance in Arabidopsis by maintaining the Ca^{2+} level and partially decreasing toxic Na^+ influx through its regulation of voltage-independent channels and NSCCs (Tyerman et al. 1997, Davenport and Tester 2000, Maathuis and Sanders 2001).

Potential roles of HvHKT1;1 for salt tolerance

We found that knock-out of *AtHKT1; 1* caused a higher accumulation of shoot Na^+ and a reduction in root Na^+ accumulation (Fig. 6g, h), which is similar to findings of a previous report (Davenport et al. 2007). Previous studies reported that overexpression of *AtHKT1;1* increased Na^+ sensitivity of the transgenic Arabidopsis plants (Rus et al. 2004, Horie et al. 2009). Similarly, constitutive expression of sorghum *SbHKT1;4* caused excessive Na^+ influx into yeast cells and Na^+ overaccumulation in Arabidopsis shoot (Wang et al. 2014). However, specific overexpression of *AtHKT1;1* in the root pericycle could enhance Na^+ exclusion from shoots to roots by increasing Na^+ influx activity into the targeted parenchyma cells, therefore enhancing salt tolerance of Arabidopsis (Møller et al. 2009). Although the root morphologies of Arabidopsis and rice are very different, cell type-specific expression of Na^+ transporters is critical for engineering salinity tolerance (Plett et al. 2010). Here, *HvHKT1;1* expression was mainly observed in the xylem walls and parenchyma cells other than epidermal cells in barley roots (Fig. 4b). A possible explanation for this phenomenon is that the root segment was taken from a 7-day-old seedling and quite close to the root cap so that the protoplasm disintegrates, and lignification was not fully completed in the young tissue. In other words, either the xylem cells may be still 'alive', or the protein remains active for staining. Unexpectedly, *HvHKT1;1* overexpression reduced shoot Na^+ accumulation in *hkt1-4*, and both root and shoot Na^+ contents in *sos1-12* and even the salt-tolerant *sos1-6* under salt stress (Fig. 6g, h), whose tolerance has been already enhanced by higher transcript levels of *sos1* (Supplementary Figs. S4c, S6). Moreover, overexpression of *HvHKT1;1* significantly reduced K^+ efflux from Arabidopsis roots under salt treatment (Fig. 7a). These results indicated that constitutive expression of *HvHKT1;1* did not increase the Na^+ influx into plant root as the Na^+ transport through HvHKT1;1 would be prevented by the presence of $[K^+]_{ext}$ (Fig. 3d), which was different from AtHKT1;1 and SbHKT1;4 (Uozumi et al. 2000, Wang et al. 2014). In addition, HvHKT1;1 is involved in Na^+ retrieval from xylem, resulting in decreased Na^+ accumulation in shoots of barley and Arabidopsis plants (Figs. 5b, 6g). Knock-down of *HvHKT1;1* led to an elevated Na^+ content in BSMV:*HvHKT1;1* barley roots (Fig. 5b), suggesting that HvHKT1;1 may take part in Na^+ relocating to the root epidermal cells for efflux. Potential Na^+ detoxification mechanisms for HvHKT1;1 are also fine-tuned by the indirect retention and re-balancing of K^+ and Ca^{2+} in root cells, which in turn enhances plant tolerance to osmotic and oxidative stresses and, eventually, improves plant salt tolerance.

Materials and Methods

Plant materials

Two cultivated barley (*Hordeum vulgare* spp. *vulgare*) genotypes CM72 and Gairdner, and two Tibetan wild barley (*Hordeum vulgare* spp. *spontaneum*) accessions XZ16 and XZ169 were used. Seeds of Arabidopsis mutants were from the Arabidopsis Biological Resource Center (Ohio State University, USA). The *hkt1-4* homozygous mutant was identified from CS6532 by reverse transcription–PCR (RT–PCR), a high-resolution multicapillary electrophoresis system (eGene HDA-GT12; Supplementary Fig. S4a, c) and Sanger sequencing. *hkt1-4* has a 16 bp deletion in the third exon of *AtHKT1;1* and was used for the complementary function study of HvHKT1;1. To determine the function of HvHKT1;1, especially in Na^+ transport, another two *sos1* mutants with transfer DNA (T-DNA) insertions were identified from SAIL_868_E01 and SALK_149947, respectively, by the T-DNA border primer and SOS1 gene-specific primers (Supplementary Fig. S4a, b). *sos1-6* was identified by a T-DNA insertion in the 5′-untranslated region (UTR) of *AtSOS1* (Supplementary Fig. S1A), resulting in higher gene transcription (Supplementary Fig. S4c). *sos1-12* had a T-DNA insertion in the 19th exon of *AtSOS1* (Supplementary Fig. S4a), leading to complete gene silencing (Supplementary Fig. S4c). We identified 77 individual Arabidopsis T_1 lines constitutively expressing *HvHKT1;1*, and five of the homozygous transgenic T_3 Arabidopsis lines including 12-5 (from mutant *hkt1-4*), 29-1/37-3 (from mutant *sos1-6*) and 59-6/77-6 (from mutant *sos1-12*) were used in the experiments (Supplementary Fig. S4d).

Plant growth

In the salt tolerance screening test, barley plants were hydroponically grown in a glasshouse following Qiu et al. (2011). Three-week-old seedlings were grown in the control or exposed to 300 mM NaCl with 100 mM daily increment. After 17 d of treatment, plants were harvested for measurement of biomass and ion content. In the *HvHKT1;1* gene expression assay, the hydroponic culture was conducted in a growth chamber (14 h light/10 h dark photoperiod, 20°C day/14°C night, 70% humidity and light intensity of 150 μmol m^{-2} s^{-1}). Seven-day-old seedlings were transferred to an aerated nutrient solution (Qiu et al. 2011) and grown for 10 d, and then subjected to 150 mM NaCl treatment. Samples were collected at 0 (as control), 2, 6, 12 and 24 h after treatment initiation.

Arabidopsis seeds were germinated for 7 d before transferring to the pots filled with autoclaved vermiculite. Plants were grown for 4 weeks under a 10 h light/14 h dark photoperiod at 23°C with a relative humidity of 60% and an irradiation of 150 μmol m^{-2} s^{-1} (Chen et al. 2012). Plants were irrigated every 3 or 4 d with 1/5 strength Murashige and Skoog (MS) salt solution (pH 6.0), or nutrient solution supplemented with 50 or 100 mM NaCl. For root elongation assay, 4-day-old seedlings were transferred to square Petri plates containing modified MS medium that was deficient in K^+ and Ca^{2+} (Rus et al. 2004). Seedlings were photographed, and root length was analyzed with RootReader2D Software.

RNA isolation, RT–PCR and quantitative real-time PCR (qRT-PCR)

Total RNA was extracted using the RNAprep pure Plant Kit, according to the manufacturer's instructions (TIANGEN). Reverse transcription was conducted according to the PrimeScript RT Reagent Kit (TAKARA). The *HvHKT1;1* coding

sequence was amplified from wild barley accession XZ16 through RT–PCR. RT–PCR was also performed for genotyping of Arabidopsis mutants and *HvHKT1;1* overexpression lines. The Arabidopsis *18S rRNA* gene was used as an internal control. qRT-PCR was performed with iQ SYBR Green Supermix, on a CFX96 Real-Time PCR Detection System (Bio-Rad). Barley *Gapdh*, *18S rRNA* and *β-tubulin* genes were used as internal references. Primers used are listed in Supplementary Table S4.

Sequence alignment and phylogenetic analysis

Full-length protein sequences of plant HKTs and fungal TRKs were used for phylogenetic analysis. Alignment of the sequences was performed by a ClustalW2 program (http://www.ebi.ac.uk/Tools/msa/clustalw2/ (June 29, 2018, date last accessed)) and a phylogenetic tree was constructed with MEGA version 7.0.14 (Kumar et al. 2016), using the Minimum Evolution algorithm (Poisson model) with 1,001 bootstrap replicates. Accession numbers and species for all sequences are listed in Supplementary Table S2.

Yeast expression and growth

HvHKT1;1 was subcloned into a *pYES2* (Invitrogen) vector and transformed into yeast strain (*Saccharomyces cerevisiae*) R5421 (*ura3-52 his3D200 leu2 D1 trp1 D1 ade2*, *trk1 D::HIS3*, *trk2 D::HIS3*, sourced from Richard F. Gaber, Northwestern University). Yeast cells were transformed using the LiAc method and selected with Ura synthetic dropout medium (Clontech). The cells were pre-cultured in liquid AP medium (Rodríguez-Navarro and Ramos 1984) containing 2% galactose and 0.6% sucrose for 24 h, and then grown on AP agar plates with additional KCl and NaCl. The initial OD_{600} of yeast culture was adjusted to 1.0, and 10 µl each from four 10-fold serial dilutions was spotted. The wild-type yeast R757 was used as positive control. Six positive transformants were selected for each heterologous expression line, and experiments were repeated twice.

Characterization of HvHKT1;1 in *Xenopus laevis* oocytes

Gene cloning, cRNA synthesis and oocyte clamp were carried out following Grefen et al. (2010) and Byrt et al. (2014). The full-length coding sequence of *HvHKT1;1* was subcloned into pGEMHE-DEST and then the recombinant plasmid was linearized by *Sbf*I-HF (New England Biolabs). cRNA was synthesized using the mMESSAGE mMACHINE T7 Kit (Ambion) following the manufacturer's instructions. cRNA (23 ng in 46 nl) or RNA-free water (as controls) was injected into *X. laevis* oocytes with a Nanoinject II microinjector (Drummond Scientific). Oocytes were incubated at 18°C in ND96 solution for 72 h and two-microelectrode voltage clamp was conducted using an Oocyte Clamp amplifier (OC-725C, Warner Instrument). Electrodes were filled with 3 M KCl. For the selectivity analyses of monovalent cations, oocytes were bathed in HMg solution containing 6 mM $MgCl_2$, 1.8 mM $CaCl_2$, 10 mM MES (pH 6.5 adjusted with bis-tris propane) and the indicated concentrations of cation-chloride salts (or various concentrations of K^+ glutamate or Na^+ glutamate). The osmolality of each solution was adjusted to 240–260 mOsmol kg^{-1} with D-mannitol using a vapor pressure osmometer (Wescor). Voltage steps were applied from +40 to −140 in 20 mV steps, with a holding potential of −20 mV. The cycle for each voltage pulse was 10 s and the currents were only recorded for the intervening 6 s as steady state. All experiments were performed at room temperature. Voltage-pulse protocols, data acquisition and analyses were performed using Henry's Electrophysiological (EP) Suite Version 3.5.1 (University of Glasgow) and SigmaPlot 12.5 software (SYSTAT).

Subcellular localization of HvHKT1;1

The *HvHKT1;1* coding sequence was subcloned into a modified binary vector pCAMBIA 1,300 housing a superfolder GFP (sGFP) that was driven by a *Cauliflower mosaic virus* (CaMV) 35S promoter. The stop codon of *HvHKT1;1* was mutagenized to generate the cassette encoding an in-frame HvHKT1;1::sGFP fusion protein (Supplementary Table S4). The plasmid was then transiently expressed in onion epidermal cells, and pm-rb CD3-1008 was used as a plasma membrane marker. Particle bombardment was conducted by Biolistic PDS-1000/He system (Bio-Rad) with 1,100 p.s.i. rupture discs under a vacuum of 27 inches of Hg, as described by He et al. (2015). The cell layers were imaged with the LSM 780 Exciter confocal laser scanning microscope (Zeiss).

Cell type localization by immunofluorescence assay

Seeds of XZ16 and XZ169 were surface-sterilized, rinsed and germinated in the dark at 20°C for 7 d using the paper towel method. Prior to sampling, the paper towel was transferred into a beaker and saturated in a solution containing 2.0 mM K^+, 0.5 mM Ca^{2+} and 150 mM Na^+ for 16 h. Ten root segments 1.5 cm in length from the apex were excised, rinsed and then fixed in FAA solution for immunostaining. The samples were embedded in paraffin and sectioned to 5 µm thickness with a microslicer (RM2016; Leica). Sections were placed on microscope slides, deparaffinized and hydrated with distilled water, and then incubated with 1 mM Tris/EDTA (pH 9.0) in a microwave oven for antigen retrieval. After three washes in phosphate-buffered saline (PBS; pH 7.4), the sections were exposed to endogenous peroxidase blocking solution (3% hydrogen peroxide) for 25 min at room temperature, washed three times with PBS and blocked with 3% (w/v) bovine serum albumin in PBS for 30 min. Slides were then incubated overnight in a humidified chamber at 4°C with mouse anti-HvHKT1;1 monoclonal antibody (1:100 dilution in PBS). A primary antibody specific to HvHKT1;1 was produced by immunizing mice (Abmart) with the peptide N-MPELESPQTSMHRF-C (positions 1–14 of HvHKT1;1). After three washes with PBS, the slides were incubated with cyanine 3- (Cy3) conjugated secondary goat anti-mouse IgG (1:300 dilution, Goodbio Technology) in a darkened humidified chamber for 45 min at room temperature. The nuclei were counterstained with 4′,6-diamidino-2-phenylindole (DAPI; Beyotime Institute of Biotechnology) for 10 min at room temperature. Samples were mounted with antifade mounting medium and examined with an inverted microscope system (Nikon, ECLIPSE TI-SR). Two or three individual fields of view per sample were captured at magnifications of ×200 and ×400.

Virus-induced gene silencing

Plasmid construction, *in vitro* transcription and rub-inoculation of BSMV-derived vectors were conducted following He et al. (2015). To silence the *HvHKT1;1* and avoid off-targeting other genes with high sequence similarity, two independent cDNA clones of BSMV:*HvHKT1;1* were generated by reverse insertion of partial cDNA fragments (H1 for +130 to +539 and H2 for +819 to −+1411 from the start codon, respectively) into the RNAγ cDNA strand. Barley plants were grown hydroponically and inoculated at the two-leaf stage. The plants were then transferred to nutrient solution supplemented with (treatment) or without (control) an additional 200 mM NaCl 14 d after inoculation. To monitor the dynamic expression of *HvHKT1;1*, the whole roots as well as shoot tissues that newly emerged after BSMV inoculation were sampled at 0, 1.5, 6.0, 24, 72 and 120 h after treatment initiation, with four biological replicates. *18S rRNA* and *β-tubulin* were used as internal controls in relative qRT-PCR (Supplementary Table S4). After 5 d salt treatment, the shoots and roots of eight seedlings were harvested for ion content measurement [inductively coupled plasma-optical emission spectrometry (ICP-OES)], and the plant tissues above the second leaf were detached from the main shoot for dry biomass measurement.

Immunoblotting assay

Immunoblotting of HvHKT1;1 was performed as described by Ye et al. (2011) with minor modifications. Membrane proteins were extracted from fresh root samples of BSMV:γ and BSMV:*HvHKT1;1* plants (XZ16) after 5 d salt treatment using ProteoExtract® Transmembrane Protein Extraction Kit (Merck Millipore Corporation), according to the manufacturer's instructions. A 10 µg aliquot of protein from each sample was loaded in the gel and SDS–PAGE was carried out with a 10% resolving gel and a 5% stacking gel at a constant voltage of 100 V for 2 h in an electrophoresis unit (Bio-Rad). The separated proteins were then transferred to a nitrocellulose transfer membrane (0.2 mm pore size, Whatman) by the Trans-Blot® SD semi-dry transfer cell (Bio-Rad) at a constant 15 V for 17 min. After blocking, the membrane was incubated with the monoclonal anti-HvHKT1;1 antibody diluted 1:500 in Western BLoT Immuno Booster Solution I (TAKARA). Actin (26F7) mouse mAb for Plants (Abmart) was used as internal reference. Goat anti-mouse horseradish peroxidase antibody (Goodbio Technology) diluted in Booster Solution II (1:5,000; TAKARA) was used as the secondary antibody. The immunoblots were developed using the Immun-Star Western C Kit (Bio-Rad) and then imaged by LAS-3000 (Fujifilm).

35S:HvHKT1;1 construction and Arabidopsis transformation

The coding sequence was subcloned into pCR8\GW\TOPO vector (Life Technologies) and sequenced. *35S:HvHKT1;1* was generated by inserting a 1,761 bp full-length coding sequence into pCambia1301 (Supplementary Table S4). The resulting construct was delivered to *Agrobacterium tumefaciens* strain GV3101 and transferred to Arabidopsis using the floral dip method (Clough and Bent 1998). T_2 transformants were grown on Petri dishes and subjected to χ^2 test for hygromycin resistance to ensure there was only single transgene segregation.

Ion content analysis

Plant tissues were collected, rinsed with distilled water, oven-dried and weighed. The samples were subjected to microwave digestion (Anton Paar, Microwave 3000), and subsequently, ion content was measured using ICP-OES (PerkinElmer, Optima 8000DV) as described by Wu et al. (2011).

Ion flux measurements

Net fluxes of K^+, H^+ and Ca^{2+} were measured non-invasively using ion-selective vibrating microelectrodes (the MIFE technique) (Chen et al. 2005, Shabala et al. 2010). Microelectrodes were filled with ion-selective cocktails (Sigma). Arabidopsis seedlings were grown on Phytagel on Petri dishes for 10–12 d before ion flux measurements. Seedlings were collected and immediately pre-incubated in a 5 ml Perspex-glass measuring chamber with 2.5 ml of control solution (0.5 mM KCl and 0.1 mM $CaCl_2$) for 1 h. K^+, H^+ and Ca^{2+} fluxes of roots in the control were measured for 10 min to ensure steady initial values before adding 50 mM NaCl. Recordings were continued for a further 30 min after the application of each treatment.

Statistical analysis

A complete random block design with at least three biological replicates was used for each experiment. Comparisons between groups were tested by one-way analysis of variance (ANOVA) and Tukey's test using the IBM SPSS Statistics Package (Version 22).

Supplementary Data

Supplementary data are available at PCP online.

Funding

This work was supported by the National Natural Science Foundation of China (grant Nos. 31501296, 31571578 and 31620103912); China Agriculture Research System (CARS-05); Chinese 1000-Plan project; and the Australian Research Council (ARC) [Discovery Early Career Researcher Award (DE1401011143)].

Acknowledgments

We thank Drs. Peidu Chen (Nanjing Agricultural University), Wanli Guo (Zhejiang Sci-Tech University), De-an Jiang and Xuechang Wu (Zhejiang University) for kindly providing vectors. We really appreciate critical comments on the manuscript from Tracey Ann Cuin (University of Tasmania), Calum Watt (Murdoch University) and Mary Williams (ASPB and University of Glasgow).

Disclosures

The authors have no conflicts of interest to declare.

References

Ali, Z., Park, H.C., Ali, A., Oh, D.H., Aman, R., Kropornicka, A., et al. (2012) *TsHKT1;2*, a HKT1 homolog from the extremophile *Arabidopsis* relative *Thellungiella salsuginea*, shows K^+ specificity in the presence of NaCl. *Plant Physiol.* 158: 1463–1474.

Bose, J., Xie, Y., Shen, W. and Shabala, S. (2013) Haem oxygenase modifies salinity tolerance in *Arabidopsis* by controlling K^+ retention via regulation of the plasma membrane H^+-ATPase and by altering SOS1 transcript levels in roots. *J. Exp. Bot.* 64: 471–481.

Byrt, C.S., Platten, J.D., Spielmeyer, W., James, R.A., Lagudah, E.S., Dennis, E.S., et al. (2007) HKT1;5-like cation transporters linked to Na^+ exclusion loci in wheat, *Nax2* and *Kna1*. *Plant Physiol.* 143: 1918–1928.

Byrt, C.S., Xu, B., Krishnan, M., Lightfoot, D.J., Athman, A., Jacobs, A.K., et al. (2014) The Na^+ transporter, TaHKT1;5-D, limits shoot Na^+ accumulation in bread wheat. *Plant J.* 80: 516–526.

Chen, M., Wang, Z., Zhu, Y., Li, Z., Hussain, N., Xuan, L., et al. (2012) The effect of *transparent TESTA2* on seed fatty acid biosynthesis and tolerance to environmental stresses during young seedling establishment in *Arabidopsis*. *Plant Physiol.* 160: 1023–1036.

Chen, Z.H., Newman, I.A., Zhou, M., Mendham, N.J., Zhang, G. and Shabala, S. (2005) Screening plants for salt tolerance by measuring K^+ flux, a case study for barley. *Plant Cell Environ.* 28: 1230–1246.

Clough, S.J. and Bent, A.F. (1998) Floral dip, a simplified method for *Agrobacterium*-mediated transformation of *Arabidopsis thaliana*. *Plant J.* 16: 735–743.

Corratgé-Faillie, C., Jabnoune, M., Zimmermann, S., Véry, A.A., Fizames, C. and Sentenac, H. (2010) Potassium and sodium transport in non-animal cells, the Trk/Ktr/HKT transporter family. *Cell. Mol. Life Sci.* 67: 2511–2532.

Davenport, R.J., Muñoz-Mayor, A., Jha, D., Essah, P.A., Rus, A. and Tester, M. (2007) The Na^+ transporter *AtHKT1;1* controls retrieval of Na^+ from the xylem in *Arabidopsis*. *Plant Cell Environ.* 30: 497–507.

Davenport, R.J. and Tester, M. (2000) A weakly voltage-dependent, non-selective cation channel mediates toxic sodium influx in wheat. *Plant Physiol.* 122: 823–834.

Epstein, E., Norlyn, J.D., Rush, D.W., Kingsbury, R.W., Kelley, D.B., Cunningham, G.A., et al. (1980) Saline culture of crops: a genetic approach. *Science* 210: 399–404.

Garciadeblás, B., Senn, M.E., Bañuelos, M.A. and Rodríguez-Navarro, A. (2003) Sodium transport and HKT transporters, the rice model. *Plant J.* 34: 788–801.

Golldack, D., Su, H., Quigley, F., Kamasani, U.R., Muñoz-Garay, C., Balderas, E., et al. (2002) Characterization of a HKT-type transporter in rice as a general alkali cation transporter. *Plant J.* 31: 529–542.

Grefen, C., Chen, Z.H., Honsbein, A., Donald, N., Hills, A. and Blatt, M.R. (2010) A novel motif essential for SNARE interaction with the K^+ channel KC1 and channel gating in Arabidopsis. *Plant Cell* 22: 3076–3093.

Haro, R., Bañuelos, M.A. and Rodríguez-Navarro, A. (2009) High-affinity sodium uptake in land plants. *Plant Cell Physiol.* 51: 68–79.

Haro, R., Bañuelos, M.A., Senn, M.E., Barrero-Gil, J. and Rodríguez-Navarro, A. (2005) HKT1 mediates sodium uniport in roots. Pitfalls in the expression of HKT1 in yeast. *Plant Physiol.* 139: 1495–1506.

Hauser, F. and Horie, T. (2010) A conserved primary salt tolerance mechanism mediated by HKT transporters, a mechanism for sodium exclusion and maintenance of high K^+/Na^+ ratio in leaves during salinity stress. *Plant Cell Environ.* 33: 552–565.

He, X., Zeng, J., Cao, F., Ahmed, I.M., Zhang, G., Vincze, E., et al. (2015) *HvEXPB7*, a novel β-expansin gene revealed by the root hair

transcriptome of Tibetan wild barley, improves root hair growth under drought stress. *J. Exp. Bot.* 66: 7405–7419.

Horie, T., Costa, A., Kim, T.H., Han, M.J., Horie, R., Leung, H.Y., et al. (2007) Rice *OsHKT2;1* transporter mediates large Na^+ influx component into K^+-starved roots for growth. *EMBO J.* 26: 3003–3014.

Horie, T., Hauser, F. and Schroeder, J.I. (2009) HKT transporter-mediated salinity resistance mechanisms in *Arabidopsis* and monocot crop plants. *Trends Plant Sci*. 14: 660–668.

Huang, S., Spielmeyer, W., Lagudah, E.S., James, R.A., Platten, J.D., Dennis, E.S., et al. (2006) A sodium transporter (HKT7) is a candidate for *Nax1*, a gene for salt tolerance in durum wheat. *Plant Physiol.* 142: 1718–1727.

Huang, S., Spielmeyer, W., Lagudah, E.S. and Munns, R. (2008) Comparative mapping of HKT genes in wheat, barley, and rice, key determinants of Na^+ transport, and salt tolerance. *J. Exp. Bot.* 59: 927–937.

Jabnoune, M., Espeout, S., Mieulet, D., Fizames, C., Verdeil, J.L., Conejero, G., et al. (2009) Diversity in expression patterns and functional properties in the rice HKT transporter family. *Plant Physiol.* 150: 1955–1971.

Kato, Y., Sakaguchi, M., Mori, Y., Saito, K., Nakamura, T., Bakker, E.P., et al. (2001) Evidence in support of a four transmembrane-pore-transmembrane topology model for the *Arabidopsis thaliana* Na^+/K^+ translocating *AtHKT1* protein, a member of the superfamily of K^+ transporters. *Proc. Natl. Acad. Sci. USA* 98: 6488–6493.

Kobayashi, N.I., Yamaji, N., Yamamoto, H., Okubo, K., Ueno, H., Costa, A., et al. (2017) OsHKT1;5 mediates Na^+ exclusion in the vasculature to protect leaf blades and reproductive tissues from salt toxicity in rice. *Plant J.* 91: 657–670.

Kumar, S., Stecher, G. and Tamura, K. (2016) MEGA7: molecular evolutionary genetics analysis version 7.0 for bigger datasets. *Mol. Biol. Evol.* 33: 1870–1874.

Maathuis, F.J. and Sanders, D. (2001) Sodium uptake in *Arabidopsis* roots is regulated by cyclic nucleotides. *Plant Physiol.* 127: 1617–1625.

Mäser, P., Eckelman, B., Vaidyanathan, R., Horie, T., Fairbairn, D.J., Kubo, M., et al. (2002c) Altered shoot/root Na^+ distribution and bifurcating salt sensitivity in Arabidopsis by genetic disruption of the Na^+ transporter AtHKT1. *FEBS Lett.* 531: 157–161.

Mäser, P., Gierth, M. and Schroeder, J.I. (2002b) Molecular mechanisms of potassium and sodium uptake in plants. *Plant Soil* 247: 43–54.

Mäser, P., Hosoo, Y., Goshima, S., Horie, T., Eckelman, B., Yamada, K., et al. (2002a) Glycine residues in potassium channel-like selectivity filters determine potassium selectivity in four-loop-per-subunit HKT transporters from plants. *Proc. Natl. Acad. Sci. USA* 99: 6428–6433.

Mäser, P., Thomine, S., Schroeder, J.I., Ward, J.M., Hirschi, K., Sze, H., et al. (2001) Phylogenetic relationships within cation transporter families of *Arabidopsis thaliana*. *Plant Physiol*. 126: 1646–1667.

Mian, A., Oomen, R.J.F.J., Isayenkov, S., Sentenac, H., Maathuis, F.J.M. and Véry, A.A. (2011) Over-expression of a Na^+- and K^+-permeable HKT transporter in barley improves salt tolerance. *Plant J.* 68: 468–479.

Møller, I.S., Gilliham, M., Jha, D., Mayo, G.M., Roy, S.J., Coates, J.C., et al. (2009) Shoot Na^+ exclusion and increased salinity tolerance engineered by cell type-specific alteration of Na^+ transport in *Arabidopsis*. *Plant Cell* 21: 2163–2178.

Munns, R. and Tester, M. (2008) Mechanisms of salinity tolerance. *Annu. Rev. Plant Biol.* 59: 651–681.

Oomen, R.J.F.J., Benito, B., Sentenac, H., Rodríguez-Navarro, A., Talón, M., Véry, A.A., et al. (2012) HKT2; 2/1, a K^+-permeable transporter identified in a salt-tolerant rice cultivar through surveys of natural genetic polymorphism. *Plant J.* 71: 750–762.

Plett, D., Safwat, G., Gilliham, M., Skrumsager Møller, I., Roy, S., Shirley, N., et al. (2010) Improved salinity tolerance of rice through cell type-specific expression of AtHKT1; 1. *PLoS One* 5: e12571.

Qiu, L., Wu, D.Z., Ali, S., Cai, S.G., Dai, F., Jin, X., et al. (2011) Evaluation of salinity tolerance and analysis of allelic function of *HvHKT1* and *HvHKT2* in Tibetan wild barley. *Theor. Appl. Genet.* 122: 695–703.

Rengasamy, P. (2010) Soil processes affecting crop production in salt-affected soils. *Funct. Plant Biol.* 37: 613–620.

Rodríguez-Navarro, A. and Ramos, J. (1984) Dual system for potassium transport in *Saccharomyces cerevisiae*. *J. Bacteriol.* 159: 940–945.

Rodríguez-Navarro, A. and Rubio, F. (2006) High-affinity potassium and sodium transport systems in plants. *J. Exp. Bot.* 57: 1149–1160.

Rus, A., Lee, B.H., Muñoz-Mayor, A., Sharkhuu, A., Miura, K., Zhu, J.K., et al. (2004) *AtHKT1* facilitates Na^+ homeostasis and K^+ nutrition in *planta*. *Plant Physiol.* 136: 2500–2511.

Sassi, A., Mieulet, D., Khan, I., Moreau, B., Gaillard, I., Sentenac, H., et al. (2012) The rice monovalent cation transporter *OsHKT2;4*, revisited ionic selectivity. *Plant Physiol.* 160: 498–510.

Shabala, S., Shabala, L., Cuin, T., Pang, J., Percey, W., Chen, Z.H., et al. (2010) Xylem ionic relations and salinity tolerance in barley. *Plant J.* 61: 839–853.

Suzuki, K., Yamaji, N., Costa, A., Okuma, E., Kobayashi, N.I., Kashiwagi, T., et al. (2016) OsHKT1;4-mediated Na^+ transport in stems contributes to Na^+ exclusion from leaf blades of rice at the reproductive growth stage upon salt stress. *BMC Plant Biol.* 16: 22.

Tyerman, S., Skerrett, M., Garrill, A., Findlay, G. and Leigh, R. (1997) Pathways for the permeation of Na^+ and Cl^- into protoplasts derived from the cortex of wheat roots. *J. Exp. Bot.* 48: 459–480.

Uozumi, N., Kim, E.J., Rubio, F., Yamaguchi, T., Muto, S., Tsuboi, A., et al. (2000) The *Arabidopsis HKT1* gene homolog mediates inward Na^+ currents in *Xenopus laevis* oocytes and Na^+ uptake in *Saccharomyces cerevisiae*. *Plant Physiol.* 122: 1249–1260.

Volkov, V. and Amtmann, A. (2006) *Thellungiella halophila*, a salt-tolerant relative of *Arabidopsis thaliana*, has specific root ion-channel features supporting K^+/Na^+ homeostasis under salinity stress. *Plant J.* 48: 342–353.

Wang, T.T., Ren, Z.J., Liu, Z.Q., Feng, X., Guo, R.Q., Li, B.G., et al. (2014) *SbHKT1;4*, a member of the high-affinity potassium transporter gene family from *Sorghum bicolor*, functions to maintain optimal Na^+/K^+ balance under Na^+ stress. *J. Integr. Plant Biol.* 56: 315–332.

Waters, S., Gilliham, M. and Hrmova, M. (2013) Plant high-affinity potassium (HKT) transporters involved in salinity tolerance, structural insights to probe differences in ion selectivity. *Int. J. Mol. Sci.* 14: 7660–7680.

Wu, D., Qiu, L., Xu, L., Ye, L., Chen, M., Sun, D., et al. (2011) Genetic variation of *HvCBF* genes and their association with salinity tolerance in Tibetan annual wild barley. *PLoS One* 6: e22938.

Yao, X.H., Horie, T., Xue, S., Leung, H.Y., Katsuhara, M., Brodsky, D.E., et al. (2010) Differential sodium and potassium transport selectivities of the rice *OsHKT2;1* and *OsHKT2;2* transporters in plant cells. *Plant Physiol*. 152: 341–355.

Ye, L.Z., Dai, F., Qiu, L., Sun, D.F. and Zhang, G.P. (2011) Allelic diversity of a beer haze active protein gene in cultivated and Tibetan wild barley and development of allelic specific markers. *J. Agric. Food Chem.* 59: 7218–7223.

Zeng, J., He, X., Wu, D., Zhu, B., Cai, S., Nadira, U.A., et al. (2014) Comparative transcriptome profiling of two Tibetan wild barley genotypes in responses to low potassium. *PLoS One* 9: e100567.